The effect of Gd substitution on the magnetic properties and hyperfine fields of melt-spun $Nd_4Fe_{77.5}B_{18.5}$ alloys

1994 J. Phys.: Condens. Matter 6 7437

(http://iopscience.iop.org/0953-8984/6/36/023)

J. Phys.: Condens. Matter 6 (1994) 7437–7444. Printed in the UK

The effect of Gd substitution on the magnetic properties and hyperfine fields of melt-spun $Nd_4Fe_{77.5}B_{18.5}$ alloys

Zhao-hua Cheng†‡, Ming-xi Mao‡, Ji-jun Sun‡§, Bao-gen Shen†, Fang-wei Wang†, Chun-li Yang‡, Fa-shen Li‡ and Yi-de Zhang‡

† State Key Laboratory of Magnetism, Institute of Physics, Chinese Academy of Sciences, Beijing 100080, People's Republic of China

‡ Department of Physics, Lanzhou University, Lanzhou 730000, People's Republic of China

§ National Laboratory for Superconductivity, Institute of Physics, Chinese Academy of Sciences, People's Republic of China

Received 5 May 1994

Abstract. The hyperfine fields (HFS) and magnetic properties of amorphous and crystallized $Gd_xNd_{4-x}Fe_{77.5}B_{18.5}$ ($0 \leqslant x \leqslant 4$) alloys have been investigated by means of magnetization measurements, zero-field spin-echo nuclear magnetic resonance (NMR) and Mössbauer effect (ME). For comparison, the x-ray diffraction (XRD) pattern of $Nd_4Fe_{77.5}B_{18.5}$ annealed at 670 °C for a short time is also presented. It is found that the Curie temperatures of amorphous alloys increase slightly on addition of Gd, but the coercive fields of crystallized alloys decrease monotonically with increasing x. NMR, ME and XRD indicate that these samples consist of Fe_3B with a body-centred tetragonal structure (BCT Fe_3B) and a small amount of α-Fe, with no $Nd_2Fe_{14}B$ and $Nd_{1.1}Fe_4B_4$ phases. Furthermore, the NMR results indicate that the ^{11}B HFS of BCT Fe_3B increase linearly from 25.3 kOe (34.7 MHz) for $x = 0$ to 26.3 kOe (36.0 MHz) for $x = 4$, but that of α-Fe does not change with increasing Gd concentration; the Mössbauer spectra (MSS) show that the relative intensity of the subspectrum corresponding to ^{57}Fe at $Fe_{III}(8g)$ sites in BCT Fe_3B is about 5% weaker than those of the other two, implying that about 5 at.% Fe atoms in this site are substituted by other atoms. According to this, it may be reasonable to assume that the R atoms enter into the BCT Fe_3B.

1. Introduction

Since 1988, there have been a large number of reports on the magnetic properties of rapidly quenched Nd–Fe–B alloys with a lower neodymium concentration. These materials exhibit a high remanence magnetization as well as an energy product and can be used as an inexpensive bonded permanent magnet [1–4]. Coehoorn *et al* [1,2] reported hard magnetic properties in the rapidly quenched $Nd_4Fe_{80}B_{20}$ alloy, which has an energy product of 11.7 MG Oe. Shen and co-workers [3–6] have also studied Nd–Fe–B systematically over a wide composition range and found a remanence magnetization of 12.5 kG, a coercive field of 3 kOe and an energy product of 13 MG Oe in $Nd_4Fe_{77.5}B_{18.5}$ alloy annealed at 670 °C for a short time. However, x-ray diffraction (XRD) results demonstrate that this sample consists of Fe_3B with a body-centred tetragonal structure (BCT Fe_3B), a small amount of α-Fe and no $Nd_2Fe_{14}B$ hard magnetic phase. A combined zero-field spin-echo nuclear magnetic resonance (NMR) and Mössbauer study was undertaken to investigate the phase components of $Nd_4Fe_{77.5}B_{18.5}$ alloys annealed at different temperatures [7]. The results are similar to those of XRD. Furthermore, the ^{11}B NMR lines corresponding to BCT Fe_3B broadens asymmetrically to the high-frequency side. We assumed that distortion of the peak

0953-8984/94/367437+08$19.50

arises because Nd atoms enter BCT Fe_3B, and the hard magnetic properties of this material originate from the presence of BCT Fe_3B containing Nd atoms. In this work, we investigate the influence of Gd substitution for Nd on the magnetic properties and hyperfine fields (HFs) of $Nd_4Fe_{77.5}B_{18.5}$ amorphous and crystallized alloys.

2. Experimental details

Iron (purity, 99.9%), neodymium (purity, 99.9%), gadolinium (purity, 99.9%) and Fe–B alloy (purity, 98.6%) were arc melted in an argon atmosphere of high purity into homogeneous buttons with the nominal composition $Nd_{4-x}Gd_xFe_{77.5}B_{18.5}$ ($0 \leqslant x \leqslant 4$). Amorphous ribbons were prepared by melt spinning in a high-purity argon atmosphere with a polished Cu drum of 20 cm diameter with a speed of 47 m s^{-1}. The thickness and the width of the ribbons were about 20 μm and 1 mm, respectively. XRD patterns confirmed the amorphous state of the ribbons. The Curie temperatures T_C of these amorphous alloys were determined by the temperature dependence of the AC susceptibility in a very weak magnetic field, less than 1 Oe. The crystallized samples were annealed at 670 °C for a short time in a steel tube in vacuum of 2×10^{-5} Torr. Hysteresis loop measurements on the heat-treated samples were carried out at room temperature using a vibrating-sample magnetometer with a maximum magnetic field of 8 kOe.

Zero-field spin-echo NMR spectra of ^{11}B and ^{57}Fe were performed at a temperature of 8 K for frequencies ranging from 20 to 60 MHz. A closed-cycle refrigerator was employed to provide this low temperature without the consumption of liquid helium. The details of the NMR experiments have been described elsewhere [8]. The Mössbauer spectra (MSs) were recorded at room temperature using a constant-acceleration spectrometer with a ^{57}Co(Pd) source. The isomer shifts (ISs) given in this paper were relative to α-Fe at room temperature. The XRD experiments were performed with Co Kα radiation.

3. Results and discussion

Figure 1 shows the Curie temperatures T_C of $Gd_xNd_{4-x}Ge_{77.5}B_{18.5}$ ($0 \leqslant x \leqslant 4$) amorphous alloys as a function of Gd concentration. It is found the Curie temperatures increase slightly with increasing x. In the case of rare-earth–iron compounds or alloys, the Curie temperature is determined by the Fe–Fe, R–Fe and R–R exchange interactions. It is commonly assumed that the Fe–Fe exchange interaction plays a predominant role and the R–R interaction can be negligible. So the effect of Gd substitution for Nd on the Curie temperatures of Nd–Gd–Fe–B amorphous alloys is not obvious. The different T_C-values for the various rare-earth compounds are mainly attributed to the effect of the R–Fe interactions on T_C. On the basis of molecular-field theory, the R–Fe interaction is proportional to the de Gennes factor $(g-1)^2J(J+1)$. The de Gennes factors of Gd and Nd are 15.8 and 1.84, respectively. So T_C increases with increasing Gd content x.

For example, figure 2 gives hysteresis loops measured at room temperature in an applied field of 8 kOe for samples with $x = 1$ and $x = 4$ annealed at 670 °C for a short time. From figure 2, one can see that a characteristic feature of these materials is the high isotropic M_r/M_s-ratio of about 0.7–0.8. For an assembly of randomly oriented non-interacting crystallites with uniaxial anisotropy, M_r/M_s is 0.5 if the magnetization is determined by a coherent amount of spin in the grains. The ratio can be even lower owing to domain formation. So the high ratio M_r/M_s of remanence magnetization to saturation

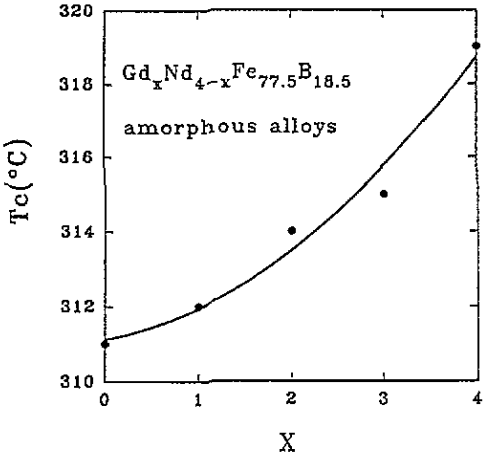

Figure 1. The Curie temperature of amorphous $Gd_xNd_{4-x}Fe_{77.5}B_{18.5}$ alloys as a function of Gd concentration x.

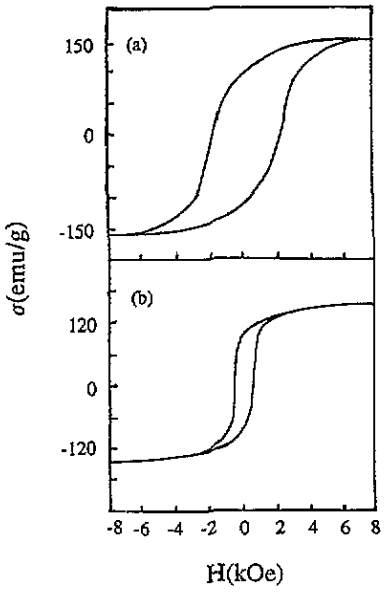

Figure 2. The hysteresis loops of crystallized $Gd_xNd_{4-x}Fe_{77.5}B_{18.5}$ alloys measured at room temperature in a field of 8 kOe: (a) for $x = 1$; (b) for $x = 4$.

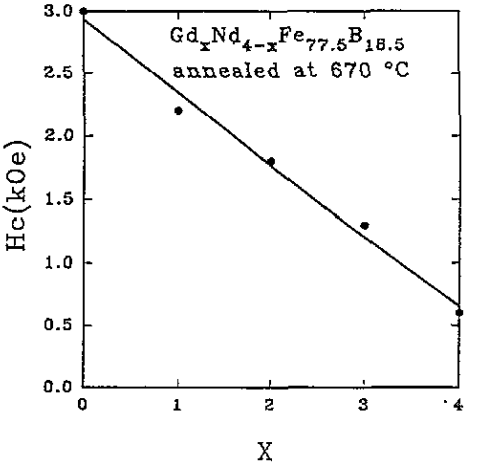

Figure 3. The coercive field at room temperature of crystallized $Gd_xNd_{4-x}Fe_{77.5}B_{18.5}$ alloys as a function Gd concentration x.

magnetization can be explained by the strong magnetic interactions between the uniaxial magnetocrystalline anisotropy BCT Fe_3B containing Nd atoms and α-Fe crystallites.

The coercive field H_c versus the Gd concentration x is shown in figure 3. H_c reduces monotonically from 3 to 0.6 kOe, as x increases from 0 to 4. For the rare-earth–iron compounds or alloys, the contribution to magnetocrystalline anisotropy arises mainly from the rare-earth sublattices. The Gd atoms have a non-orbit magnetic moment, and consequently no contribution to the magnetocrystalline anisotropy. Thus, H_c decreases on the addition of Gd.

Figure 4 illustrates the XRD patterns of $Nd_4Fe_{77.5}B_{18.5}$ alloys annealed at 670 °C for a

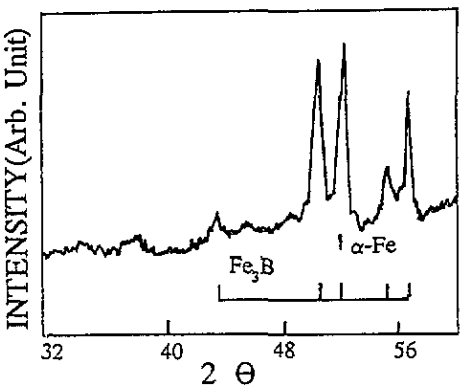

Figure 4. XRD pattern of $Nd_4Fe_{77.5}B_{18.5}$ alloy annealed at 670 °C for a short time.

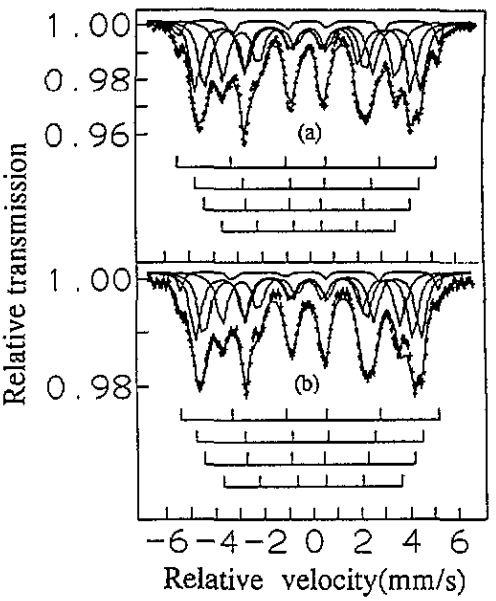

Figure 5. The Mössbauer spectra of (a) $Nd_4Fe_{77.5}B_{18.5}$ and (b) $Gd_4Fe_{77.5}B_{18.5}$ alloys annealed at 670 °C for a short time.

short time. It can be seen that this sample contains BCT Fe_3B and a few per cent of α-Fe, with no trace of the 2:14:1 phase. The MSs demonstrate that the addition of Gd does not change the phase compositions (figure 5). These results are consistent with those of XRD. The MS and XRD pattern of $Nd_3Fe_{81}B_{16}$ also give the same result [9, 10]. The hyperfine parameters of BCT Fe_3B and α-Fe obtained from fitting MSs are summarized in table 1.

Table 1. Mössbauer fitting parameters of $Nd_4Fe_{77.5}B_{18.5}$ and $Gd_4Fe_{77.5}B_{18.5}$ annealed at 670 °C for a short time.

Sample	Component	Intensity (%)	Linewidth (mm s^{-1})	IS (mm s^{-1})	QS (mm s^{-1})	HF (T)
$Nd_4Fe_{77.5}B_{18.5}$	α-Fe	5.6	0.26	0	0.02	33.3
	BCT Fe_3B	(I) 33.2	0.51	0.06	0.00	28.8
		(II) 33.2	0.51	−0.01	0.04	26.4
		(III) 28.0	0.51	0.08	0.02	22.4
$Gd_4Fe_{77.5}B_{18.5}$	α-Fe	4.6	0.26	0	0.08	33.2
	BCT Fe_3B	(I) 34.2	0.52	0.06	−0.01	28.8
		(II) 34.2	0.52	−0.01	0.06	26.5
		(III) 27.0	0.52	0.09	0.03	22.4

Figure 6 indicates the NMR spectra measured at 8 K for the heat-treated samples. The very weak peak centred at 46.7 MHz is associated with ^{57}Fe nuclei in α-Fe. Since the concentration of α-Fe in these samples is very small (about 5 at.%) and the natural abundance of ^{57}Fe nuclei is only about 2.2%, the ^{57}Fe signal is thus too weak to be detected by NMR in the samples with $x = 0$ and $x = 4$. In agreement with the XRD and Mössbauer results, NMR

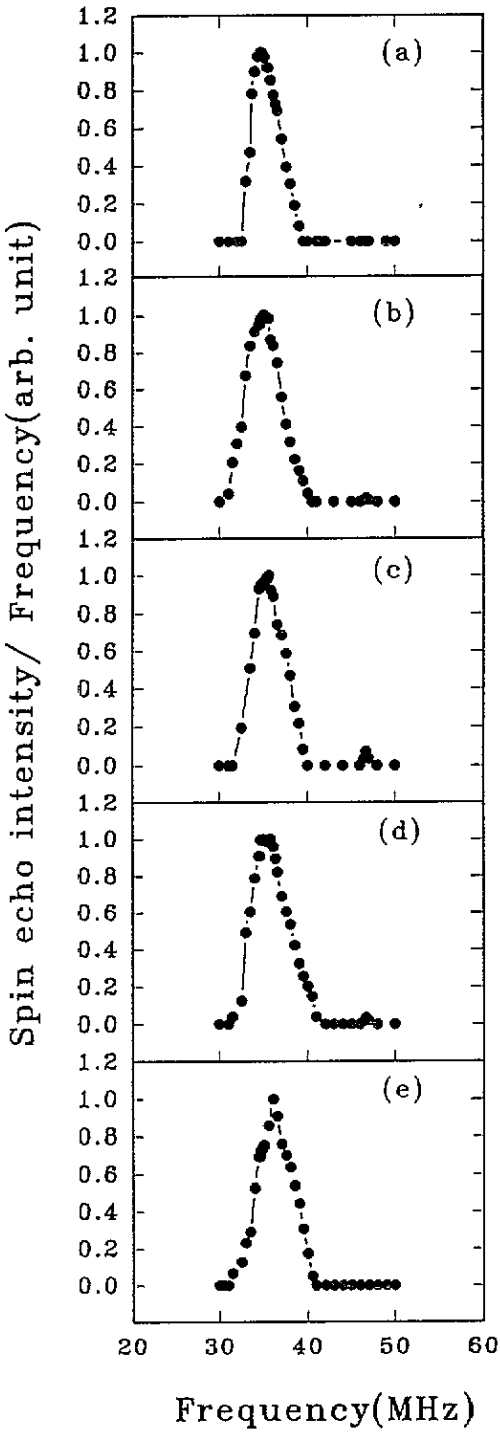

Figure 6. The spin-echo NMR spectra of crystallized $Gd_4Nd_{4-x}Fe_{77.5}B_{18.5}$ alloys: (a) for $x = 0$; (b) for $x = 1$; (c) for $x = 2$; (d) for $x = 3$; (e) for $x = 4$.

spectra also show that these samples do not contain the $Nd_2Fe_{14}B$ (2:14:1) hard magnetic phase.

It is possible that the atomic ordering in the 2:14:1 lattice may still be far from perfect and its grain size is too small to be resolved by XRD, but both NMR and ME can obtain the information concerning the nearest-neighbour environment of the detected nuclei. When a certain short-range order exists in the nearest-neighbours of the B atoms, about 10–100 Å, it can be detected by NMR and ME. In this way, NMR and ME can be utilized to identify the phase compositions whose dimensions are too small for XRD techniques. On the one hand, although B atoms are not the major component present in the 2:14:1 phase, the natural abundance of ^{11}B is about 80.8%. Furthermore, the zero-field spin-echo NMR signal comes primarily from domain walls in a polycrystalline ferromagnetic material and has a larger enhancement factor than that arising from the domain. When some amount of the 2:14:1 phase appears, the ^{11}B NMR signal can be easily detected. For small particles whose sizes are smaller than the critical size of a single domain, NMR is more difficult to observe than multiple-domain NMR because of the smaller signal intensity [11], but Mössbauer measurements are not influenced by the difference between a domain and a domain wall. On the other hand, one should note that there is a much smaller possibility that the signal of the $Nd_2Fe_{14}B$ phase overlaps that of BCT Fe_3B. For NMR, the difference between ^{11}B and ^{57}Fe hyperfine fields in BCT Fe_3B and $Nd_2Fe_{14}B$ is very large. For Mössbauer experiments a subspectrum with an average hyperfine field of 30.1 T for $Nd_2Fe_{14}B$ does not appear between the hyperfine field of 33.1 T for α-Fe and the hyperfine field of 28.8 T for the first subspectrum of BCT Fe_3B. Thus, it can be concluded that the 2:14:1 phase is not present in these samples.

On the basis of XRD and MS results, the intense peaks in figure 6, e.g. centred at 34.7 MHz in figure 6(a), 35.2 MHz in figure 6(b), 35.5 MHz in figure 6(c), 35.7 MHz in figure 6(d) and 36.0 MHz in figure 6(e), are assigned to the ^{11}B resonance signals in BCT Fe_3B. For the sample with $x = 0$, the strong line centred at 34.7 MHz is the characteristic peak of BCT Fe_3B, but it broadens asymmetrically to the high-frequency side. It is noteworthy that the ^{11}B NMR peaks corresponding to the BCT Fe_3B shift from 34.7 MHz (25.3 kOe) for $x = 0$ to 36.0 MHz (26.3 kOe) for $x = 4$ on the addition of Gd.

It is known that both NMR and ME, the hyperfine interaction techniques, can provide information concerning the local neighbourhood of the resonant nuclei. It can distinguish between lattice sites which are magnetically, atomically or electronically inequivalent. For the Fe–B-based amorphous and/or crystalline alloys, B atoms are always located in the centre of a trigonal prism formed by the nearest Fe atoms [12]. When some fluctuations exist in the nearest neighbours of the B atoms, they are bound to influence the electronic structure of B atoms and, consequently, change the hyperfine field and its distribution at B sites. For NMR experiments, the change manifests the variety of resonance lines. If the change is significant, the NMR peak will be shifted or a new resonant peak will appear. If not, the spectrum will broaden or distort. The fact that the ^{11}B hyperfine field increases with increasing x can be explained by R atoms entering BCT Fe_3B.

As they are different from the NMR results, MSs indicate that the influence of R atoms on the ^{57}Fe HFs in BCT Fe_3B is not obvious. The ^{57}Fe hyperfine parameters in BCT Fe_3B are determined from multi-phase samples, giving rise to some uncertainty. Typical uncertainties in Fe–B alloys are as follows: intensity, $\pm 1\%$, hyperfine field, ± 2 kOe; isomer shift, ± 0.3 mm s^{-1}; quadrupole splitting, ± 0.04 mm s^{-1} [13]. The fact that the Mössbauer experiment does not show the ^{57}Fe HF change means that it is less than ± 2 kOe. However, the MSs indicate that the relative intensity of the third subspectrum corresponding to the Fe_{III} (8g) site of BCT Fe_3B is about 5% weaker than those of the other two; this value of

5% is much larger than the experimental error. It is commonly assumed that the recoil-free fraction factor is similar for the three Fe sites of BCT Fe_3B and the relative intensity is proportional to the on-site Fe atom occupancies. This result means that some Fe atoms in this site are substituted by R atoms.

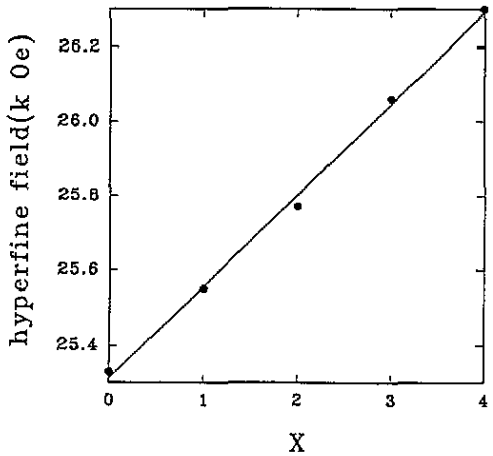

Figure 7. The hyperfine field at B sites in BCT Fe_3B versus Gd concentration in $Gd_xNd_{4-x}Fe_{77.5}B_{18.5}$ alloys.

Figure 7 shows the ^{11}B HF in BCT Fe_3B as a function of the Gd concentration x; it is approximately a linear relationship between the HF and the Gd concentration. Owing to the non-magnetic B atoms, the contribution to HF at B sites in R–Fe–B compounds and/or alloys arises mainly from the transferred hyperfine field (THF(B)). The THF(B) is proportional to the number of nearest-neighbour magnetic atoms and their magnetic moment [14]. The coupling between Nd and Fe is ferromagnetic while that between Gd and Fe is antiferromagnetic, but both Gd and Nd increase the hyperfine field at B sites. The fact that both Gd and Nd shift the peak in the same direction means that the R atom contribution to THF(B) comes from the magnetic moment of Nd and Gd via polarization of conduction electrons.

4. Conclusions

(1) The substitution of Gd for Nd increases slightly the Curie temperatures of amorphous alloys. However, the coercive fields of crystallized alloys decrease with increasing Gd concentration.

(2) The addition of Gd causes an increase in the ^{11}B hyperfine field in BCT Fe_3B but does not influence that of α-Fe. This can be explained by the R atoms entering BCT Fe_3B.

(3) The origin of hard magnetic properties in rapidly quenched Nd–Fe–B with a low Nd concentration is not related to the existence of the 2:14:1 magnetically hard phase, but to BCT Fe_3B containing Nd atoms.

Acknowledgments

This work was supported by the National Natural Science Foundation of China and State Key Laboratory of Magnetism, Institute of Physics, Chinese Academy of Sciences.

References

[1] Coehoorn R, Mooij D B, Duchateau J P W B and Buschow K H J 1988 *J. Physique Coll.* **49** C8 669
[2] Coehoorn R, de Mooij D B and de Waard C 1990 *J. Magn. Magn. Mater.* **80** 101
[3] Shen B G, Yang L Y, Zhang J X, Gu B X, Ning T S, Wo F, Zhao J G, Guo H Q and Zhan W S 1990 *Solid State Commun.* **74** 893
[4] Shen B G, Zhang J X, Yang L Y, Wo F, Ning T S, Ji S Q, Zhao J G, Guo H Q and Zhan W S 1990 *J. Magn. Magn. Mater.* **89** 195
[5] Yang L Y, Shen B G, Zhang J X, Wo F, Ning T S, Zhao J G, Guo H Q and Zhan W S 1990 *J. Less-Common Met.* **166** 189
[6] Zhang J X, Shen B G, Yang L Y and Zhan W S 1990 *Phys. Status Solidi* a **122** 651
[7] Mao M X, Yang C L, Cheng Z H, Zhang Y D, Shen B G, Yang L Y and Li F S 1992 *J. Phys.: Condens. Matter* **4** 9147
[8] Ge S H, Mao M X, Chen G L, Cheng Z H, Zhang C L, Zhang Y D, Hines W A and Budnick J I 1992 *Phys. Rev.* B **45** 4695
[9] Gu B X, Li F S, Shen B G, Zhai H R and Methfessel S 1990 *Hyperfine Interact.* **55** 961
[10] Gu B X, Zhai H R and Shen B G 1990 *Phys. Rev.* B **42** 10 648
[11] Zhang Y D, Budnick J I, Ford J C and Hines W A 1991 *J. Magn. Magn. Mater.* **100** 13
[12] Gaskell P H 1981 *Nature* **289** 474
[13] Sanchez F H, Budnick J I, Zhang Y D, Hines W A and Choi M 1986 *Phys. Rev.* B **34** 4738
[14] Zalesskij A V and Zheludev I S 1976 *At. Energy Rev.* **141** 133